20. Seto, H., Noda, Y. & Yamada, Y. Precursor phenomena at martensitic phase transition in Fe-Pd alloy. II. Diffuse scattering and embryonic fluctuations. *J. Phys. Soc. Jpn* **59,** 978–986 (1990).
21. Ferrari, V., Towler, M. & Littlewood, P. B. Oxygen stripes in $La_{0.5}Ca_{0.5}MnO_3$ from ab initio calculations. *Phys. Rev. Lett.* **91,** 227202 (2003).
22. Lynn, J. W. *et al.* Unconventional ferromagnetic transition in $La_{1-x}Ca_xMnO_3$. *Phys. Rev. Lett.* **76,** 4046–4049 (1996).
23. Lynn, J. W. *et al.* Magnetic, structural, and spin dynamical properties of $La_{1-x}Ca_xMnO_3$. *J. Appl. Phys.* **81,** 5488–5490 (1997).
24. Levy, P., Parisi, F., Granja, L., Indelicato, E. & Polla, G. Novel dynamical effects and persistent memory in phase separated manganites. *Phys. Rev. Lett.* **89,** 137001 (2002).
25. Tokura, Y., Kuwahara, H., Moritomo, Y., Tomioka, Y. & Asamitsu, A. Competing instabilities and metastable states in $(Nd,Sm)_{1/2}Sr_{1/2}MnO_3$. *Phys. Rev. Lett.* **76,** 3184–3187 (1996).
26. Kiryukhin, V. *et al.* An X-ray induced insulator metal transition in a magnetoresistive manganite. *Nature* **386,** 813–815 (1997).
27. Fiebig, M., Miyano, K., Tomioka, Y. & Tokura, Y. Visualization of the local insulator-metal transition in $Pr_{0.7}Ca_{0.3}MnO_3$. *Science* **280,** 1925–1928 (1998).
28. Chen, C. H. & Cheong, S.-W. Commensurate to incommensurate charge ordering and its real-space images in $La_{0.5}Ca_{0.5}MnO_3$. *Phys. Rev. Lett.* **76,** 4042–4045 (1996).
29. Lookman, T., Shenoy, S. R., Rasmussen, K. Ø., Saxena, A. & Bishop, A. R. Ferroelastic dynamics and strain compatibility. *Phys. Rev. B* **67,** 024114 (2003).
30. Rodriguez-Martinez, L. M. & Attfield, J. P. Cation disorder and size effects in magnetoresistive manganese oxide perovskites. *Phys. Rev. B* **54,** R15622–R15625 (1996).

Acknowledgements We thank A. Saxena for discussions. The work was supported by the US DOE.

Competing interests statement The authors declare that they have no competing financial interests.

Correspondence and requests for materials should be addressed to K.H.A. (ahn@lanl.gov).

Onset of heterogeneous crystal nucleation in colloidal suspensions

A. Cacciuto, S. Auer* & D. Frenkel

FOM Institute for Atomic and Molecular Physics, Kruislaan 407, 1098 SJ Amsterdam, The Netherlands

* Present address: Department of Chemistry, Cambridge University, Lensfield Road, Cambridge, CB2 1EW, UK

The addition of small 'seed' particles to a supersaturated solution can greatly increase the rate at which crystals nucleate. This process is understood, at least qualitatively, when the seed has the same structure as the crystal that it spawns[1,2]. However, the microscopic mechanism of seeding by a 'foreign' substance is not well understood. Here we report numerical simulations of colloidal crystallization seeded by foreign objects. We perform Monte Carlo simulations to study how smooth spherical seeds of various sizes affect crystallization in a suspension of hard colloidal particles. We compute the free-energy barrier associated with crystal nucleation[3,4]. A low barrier implies that nucleation is easy. We find that to be effective crystallization promoters, the seed particles need to exceed a well-defined minimum size. Just above this size, seed particles act as crystallization 'catalysts' as newly formed crystallites detach from the seed. In contrast, larger seed particles remain covered by the crystallites that they spawn. This phenomenon should be experimentally observable and can have important consequences for the control of the resulting crystal size distribution.

Ostwald's 1897 paper on crystal nucleation[1] contains an interesting remark in the introduction. After explaining that supercooled liquids can be made to crystallize by the introduction of a small seed crystal, Ostwald writes: "I am not aware of any experiments to determine the smallest amount of solid that is needed to make this procedure [that is, the crystallization] succeed".

More than a century has passed since then, and much has been learned about the process of crystal nucleation. But part of the question that Ostwald posed remains unanswered. The classical theory of nucleation provides a natural explanation of why a seed crystal facilitates crystal nucleation[2]: in order to grow, crystallites of the stable phase need to exceed a critical size. Crystallites that are smaller than this 'critical nucleus' dissolve again, crystallites that are larger can grow to a macroscopic size. In the absence of a seed, a rare, spontaneous fluctuation is needed to form a crystal nucleus that exceeds the critical size. However, crystallization can proceed spontaneously if we add a seed crystal that is larger than the critical nucleus to the metastable liquid phase.

But crystallization can also be induced by introducing foreign substances. And for that case, the answer to Ostwald's question is not known. Here we use computer simulations to study how very small foreign objects ('nano-dirt') influence the rate of crystal nucleation. In particular, we consider the effect of spherical seed particles on the crystallization of uncharged, spherical colloids.

First, we consider the effect of a flat wall on crystal nucleation. On an atomic scale, no wall is perfectly flat. But it is relatively straightforward to study colloidal crystallization on surfaces that are flat on the scale of a colloidal particle (50 nm, or more). Experiments[5–7] and simulations[8] show that such a flat wall speeds up colloidal crystallization by many orders of magnitude. Next, consider a smooth, spherical object of finite size. Clearly, if the object is very large, its effect should be similar to that of a hard wall. At the other limit, where the object has the same size as the colloids in the system, the object should have no effect on the nucleation rate.

One might expect that nucleation speeds up monotonically with the size of the spherical seed, but this is not true. Because crystals cannot grow on spheres without generating topological defects[9,10], nucleation of spherical particles on, or near, a sphere with a different size is inhibited. This shows up dramatically in the increase of the crystal nucleation barrier in a system of polydisperse hard spheres[11]. Yet, if we introduce only a single, mismatched sphere in the liquid, then the effect on nucleation is minimal: true, nucleation does not take place very close to this sphere, but the homogeneous nucleation in the rest of the volume is unaffected. To discover the minimum size of a spherical seed that can affect the rate of crystal nucleation,

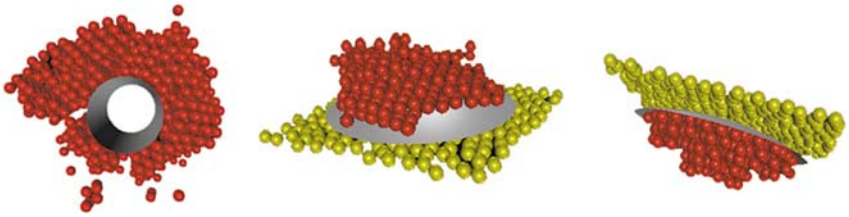

Figure 1 The spontaneous crystallizations of hard-sphere colloids on seed particles. The seed particles are a cylinder ($R_s = 3\sigma$, at $\phi = 0.523$) and a spherical cap ($R_s = 60\sigma$, at $\phi = 0.513$). The middle and right images show nucleation on the convex and on the concave sides of a spherical seed, respectively. To distinguish between the two cases, we cover the bottom (for $\kappa > 0$) or top (for $\kappa < 0$) of the spherical caps with a disordered template to prevent crystallization on that side of the seed.

we performed Monte Carlo numerical simulations of a system of monodisperse hard colloids with diameter σ containing a seed of radius R_s at its centre and systematically explored the effect of a wide range of seed sizes.

Spherical seeds with large radii ($R_s > 10\sigma$) can be studied in principle, but the computational effort quickly becomes prohibitive. To alleviate this problem, we performed simulations in which we used, as a seed, only part of the surface of a sphere with a large radius of curvature.

As a first test, we studied nucleation on a flat, circular template (infinite radius limit) with surface area $A = 150\sigma^2$ in a cubic box containing 5,632 hard spheres. The volume fraction of colloids in the liquid at freezing is $\phi^{l}_{coex} = 0.494$. In our simulations, we quickly compressed the fluid to a volume fraction $\phi = 0.513$ (reduced pressure $P\sigma^3/k_BT = 14$ where k_B is the Boltzmann constant and T is absolute temperature). At this pressure, the rate of homogeneous crystal nucleation is vanishingly small, yet, as expected[8], crystallization occurred immediately on the circular template.

Subsequently, we studied crystallization on a series of seeds, all with the same area, but with radii ranging from $R_s = 150\sigma$ to $R_s = 10\sigma$. We detected the onset of crystallization on both the convex and the concave sides of these seeds (Fig. 1). As can be seen in Fig. 2, higher pressures are needed to induce crystallization on the more strongly curved templates. Figure 2 shows that crystallization on a spherical template takes place more readily on the convex than on the concave side. The excess pressure ΔP, that is, the pressure at which crystallization sets in on a curved surface minus the corresponding pressure for a flat surface[8], appears to scale as $\Delta P \approx \kappa^{\alpha}$, where $\kappa \equiv R_s^{-1}$. A fit to the simulation data yielded $\alpha = 0.7(1)$.

We also studied seeded crystal nucleation on cylindrical templates and observed a similar scaling relation between the excess pressure at crystallization and the radius of curvature (see Fig. 2). However, for cylinders crystallization consistently takes place at lower pressures than for spheres. The observed behaviour can be described, at least qualitatively, by an extension of classical nucleation theory that takes into account the free-energy cost of elastic deformations (A.C. and D.F., manuscript in preparation).

At a pressure $P\sigma^3/k_BT = 16$ ($\phi = 0.5277$), we could study crystal nucleation on a complete spherical seed. At this pressure, the barrier for homogeneous nucleation ($\Delta G \approx 28k_BT$) is still high enough to rule out spontaneous crystallization in the bulk, and the size of the critical nucleus, $n_c \approx 110$, is sufficiently small to neglect finite size effects. We considered a system consisting of 12,167 particles and we introduced complete spherical seeds of radius $R_s = 4\sigma$, 5σ, 6σ and 7σ.

Using the umbrella-sampling techniques that we have developed[3,4], we estimated ΔG, the height of the crystal nucleation barrier, for the various spherical seeds (see Fig. 3). In the same figure, we also show the barrier for homogeneous nucleation. For a seed with radius $R_s = 4\sigma$, we find that crystal nuclei typically form in the bulk, rather than on the seed. Hence, spheres of this size are not crystallization promoters.

Seeded nucleation starts with a spherical shell of radius $R_s \simeq 5\sigma$: very small nuclei appear on the seed surface. These tend to grow radially outward until they detach and move away into the bulk (see Fig. 4). Although this seed clearly affects the crystal nucleation pathway, it hardly affects the height of the nucleation barrier. As can be seen from Fig. 3, larger seeds do lower this barrier. However, the size of the critical nucleus is hardly sensitive to the radius of the seed. This may be understood by inspecting the pathway for nucleation followed in this case (see Fig. 4).

Figure 4 shows that small nuclei grow on the seed. As they grow, the presence of a curved substrate makes it difficult to maintain an unstrained structure. At some stage, the precritical nuclei break away from the surface, and the critical nucleus is only formed in the bulk. This nucleus is therefore similar to the one observed in homogeneous nucleation. As each crystal nucleus detaches from it, the seed again becomes free to produce a new crystal—it can therefore act as an 'assembly line' for crystal nuclei (in the same way that boiling chips produce many small bubbles). Note that this will not happen when the seed is a crystal of the same material. This has important consequences for the size distribution of crystallites formed in heterogeneous nucleation: large, nearly flat seeds tend to produce one single crystal that grows to macroscopic size. But intermediate size, foreign seeds keep on producing crystal nuclei. As a consequence, the number of crystallites will be much larger than

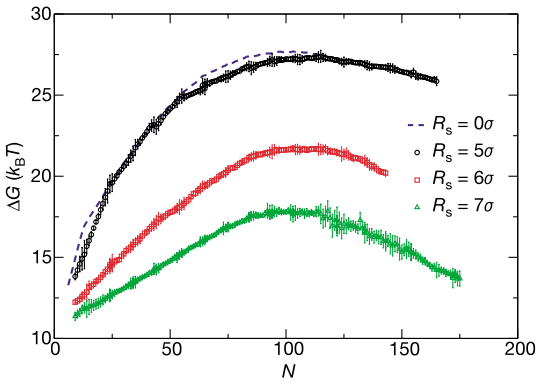

Figure 3 Free-energy barriers for crystal nucleation in a system of hard spheres with a smooth spherical seed. The seed has radii $R_s = 5\sigma$, 6σ and 7σ. The dashed curve represents the homogeneous nucleation barrier.

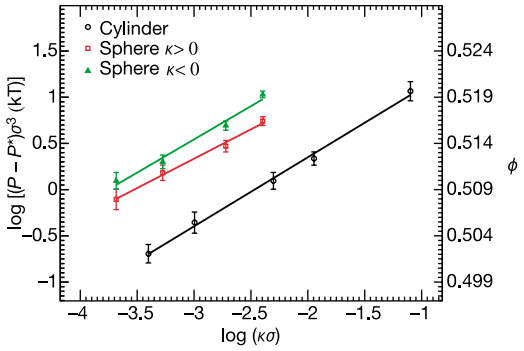

Figure 2 Plot of the smallest pressure P that causes complete crystallization as a function of the seed curvature κ. (Minus $P^* = 12.2$, representing the 'flat wall' limit.) The curves refer to the cylinder and the convex ($\kappa > 0$) and concave ($\kappa < 0$) sides of the spherical seed, as indicated. On the right axis, we show the corresponding volume fractions ϕ.

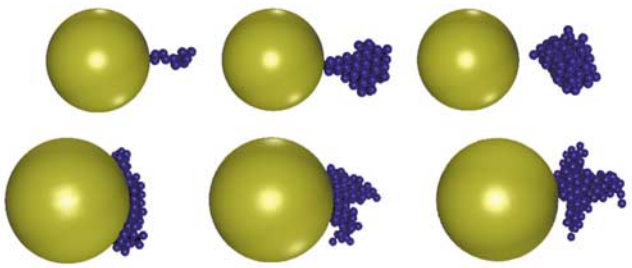

Figure 4 Snapshot sequence of crystal nucleation on spherical seeds. The seeds have radii $R_s = 5\sigma$ (top) and 7σ (bottom). From left to right the sizes of the nuclei are, respectively, $N \simeq 10$, $\simeq 50$ and $\simeq 100$ for the sphere of radius $R_s = 5\sigma$ and $N \simeq 60$, $\simeq 80$ and $\simeq 120$ for the sphere of radius $R_s = 7\sigma$. The above phenomenon should be observable in confocal microscopy studies of seeded crystallization in a colloidal suspsension.

the number of seeds and the result is that the final crystallites will be small. In many industrial processes, the control of crystallite size is important. The present work suggests that a careful selection of the size of the crystallization promoter can be of crucial importance.

Real-space imaging techniques, such as the ones used to study crystallization in colloidal suspensions[12], could be used to study seeded crystal nucleation in real colloidal systems. In such experiments, relatively large colloidal beads (spheres) or glass fibres (cylinders) could be introduced in a supersaturated solution of monodisperse, 'hard sphere' colloids. Crystallization should take place readily on the larger seeds. Owing to gravity, crystal nuclei that detach from the seed should sediment away from it. This should make it easier to image subsequent crystal nucleation events on the same seed. □

Received 9 September 2003; accepted 3 February 2004; doi:10.1038/nature02397.

1. Ostwald, W. F. Studien uber die Bildung und Umwandlung fester Korper. *Z. Phys. Chem.* **22,** 289–302 (1897).
2. Kelton, K. E. in *Solid State Physics* (eds Ehrenreich, H. & Turnbull, D.) Vol. 45 (Academic, New York, 1991).
3. ten Wolde, P. R., Ruiz-Montero, M. J. & Frenkel, D. Numerical calculation of the rate of crystal nucleation in a Lennard-Jones system at moderate undercooling. *J. Chem. Phys.* **104,** 9932–9947 (1996).
4. Auer, S. & Frenkel, D. Quantitative prediction of crystal nucleation rates for spherical colloids: A computational approach. *Annu. Rev. Phys. Chem.* **55,** (2004).
5. Kose, A. & Hachisu, S. Ordered structure in weakly flocculated monodisperse latex. *J. Colloid Interf. Sci.* **55,** 487–498 (1976).
6. Dinsmore, A., Warren, P., Poon, W. & Yodh, A. Fluid-solid transitions on walls in binary hard-sphere mixtures. *Europhys. Lett.* **40,** 337–342 (1997).
7. Kaplan, P., Rouke, J., Yodh, A. & Pine, D. Entropically driven surface phase separation in binary colloidal mixtures. *Phys. Rev. Lett.* **72,** 582–585 (1994).
8. Auer, S. & Frenkel, D. Line tension controls wall-induced crystal nucleation in hard-sphere colloids. *Phys. Rev. Lett.* **91,** 015703 (2003).
9. Euler, L. *Opera Omnia* Series i, Vol. 26 (Orell Füssli, Zurich, 1953).
10. Hilton, P. & Pederson, J. The Euler characteristic and Pólya's dream. *Am. Math. Mon.* **103,** 121–131 (1996).
11. Auer, S. & Frenkel, D. Suppression of crystal nucleation in polydisperse colloids due to increase of the surface free energy. *Nature* **413,** 711–713 (2001).
12. Gasser, U., Weeks, E. R., Schofield, A., Pussey, P. N. & Weitz, D. A. Real-space imaging of nucleation and growth in colloidal crystallization. *Science* **292,** 258–262 (2001).

Acknowledgements The work of the FOM Institute is part of the research program of FOM and is made possible by financial support from the Netherlands Organization for Scientific Research (NWO).

Competing interests statement The authors declare that they have no competing financial interests.

Correspondence and requests for materials should be addressed to A.C. (cacciuto@amolf.nl).

Mass and volume contributions to twentieth-century global sea level rise

Laury Miller[1] **& Bruce C. Douglas**[2]

[1]*Laboratory for Satellite Altimetry, NESDIS, NOAA, Silver Spring, Maryland 20910, USA*
[2]*Laboratory for Coastal Research, Florida International University, Miami, Florida 33199, USA*

The rate of twentieth-century global sea level rise and its causes are the subjects of intense controversy[1–7]. Most direct estimates from tide gauges give 1.5–2.0 mm yr^{-1}, whereas indirect estimates based on the two processes responsible for global sea level rise, namely mass and volume change, fall far below this range. Estimates of the volume increase due to ocean warming give a rate of about 0.5 mm yr^{-1} (ref. 8) and the rate due to mass increase, primarily from the melting of continental ice, is thought to be even smaller. Therefore, either the tide gauge estimates are too high, as has been suggested recently[6], or one (or both) of the mass and volume estimates is too low. Here we present an analysis of sea level measurements at tide gauges combined with observations of temperature and salinity in the Pacific and Atlantic oceans close to the gauges. We find that gauge-determined rates of sea level rise, which encompass both mass and volume changes, are two to three times higher than the rates due to volume change derived from temperature and salinity data. Our analysis supports earlier studies that put the twentieth-century rate in the 1.5–2.0 mm yr^{-1} range, but more importantly it suggests that mass increase plays a larger role than ocean warming in twentieth-century global sea level rise.

At the time of the second IPCC assessment in 1995[9], there seemed to be little controversy regarding global sea level rise (GSLR). Most gauge estimates fell in the range 1.5–2.0 mm yr^{-1}. Most of this rise was thought to result from ocean warming, with the rest due to melting of continental ice. However, by the third IPCC assessment in 2001[1], this consensus view had collapsed: new and better estimates of ocean warming had reduced the volume increase component to about 0.5 mm yr^{-1} (ref. 8), and the mass component was thought to be even smaller. This left a large unexplained gap between direct and indirect estimates of GSLR, now known as the 'attribution problem'.

Two recent studies offer opposing solutions to this dilemma. Cabanes *et al.*[6] argue that gauge rates are 2–3 times too high because the gauges happen to be located in areas of abnormally high ocean warming. They arrive at this result by comparing gauge-derived sea level trends with those obtained from objectively interpolated hydrographic measurements, concluding that the true rate of GSLR is actually 0.5–1.0 mm yr^{-1}, mostly due to ocean warming. This solution provides a way out of the attribution problem, but implies a huge acceleration of GSLR in the 1990s if recent satellite altimetric estimates of ~2.5 mm yr^{-1} (ref. 10) are to be believed. Alternatively, Antonov *et al.*[7] suggest that the problem may be solved by revising upward the mass component estimate. They show that the oceans are freshening at a rate equivalent to the addition of 1.4 mm yr^{-1} of fresh water, approximately the value needed to bring the mass plus volume rate close to the gauge rate. However, this solution assumes a continental ice source rather than floating ice, a key point that they are unable to demonstrate.

Here we present a simple approach to the problem of distinguishing between mass and volume contributions to GSLR. We identify large areas in the Pacific and Atlantic oceans that are either bounded by, or adjacent to, several gauge sites exhibiting similar trends and variability. For those regions, we compare average gauge trends (which reflect both mass and volume change) with average dynamic height trends (which reflect only volume change), with the added distinction that we use raw rather than interpolated hydrographic data. In most areas, the difference between raw and interpolated data are unimportant. However, as shown below, the interpolated data used by Cabanes *et al.*[6] contains errors near the Gulf Stream large enough to cause their average warming estimate for the gauge sites to be biased upward by a factor of 2–3. In contrast, we find no evidence that the gauges are located in regions of abnormally high warming.

We begin in the Eastern Pacific in a region bounded by gauge sites at Honolulu, San Francisco, San Diego, and Balboa, Panama (map inset, Fig. 1). This region has several characteristics that make it ideal for this study: low mesoscale variability, narrow continental margins, large numbers of hydrographic observations, and long (>90 yr) gauge records. Figure 1 presents ~19,000 dynamic height anomaly observations relative to 1,000 m, their 5-yr running means, and 5-yr running means of the four gauge records. Although the hydrographic data appear noisy in this plot, their r.m.s., 6.7 cm, is comparable to satellite altimeter determinations of sea level variability in this relatively quiet part of the global ocean[11]. A linear